Unstructured RNA Is a Substrate for tRNase Z[†]

Hirotaka S. Shibata, Asako Minagawa, Hiroaki Takaku, Masamichi Takagi, and Masayuki Nashimoto*

Department of Applied Life Sciences, Niigata University of Pharmacy and Applied Life Sciences,
Niigata, Niigata 956-8603, Japan

ABSTRACT: tRNase Z, which exists in almost all cells, is believed to be working primarily for tRNA 3′ maturation. In *Escherichia coli*, however, the tRNase Z gene appears to be dispensable under normal growth conditions, and its physiological role is not clear. Here, to investigate a possibility that *E. coli* tRNase Z cleaves RNAs other than pre-tRNAs, we tested several unstructured RNAs for cleavage. Surprisingly, all these substrates were cleaved very efficiently at multiple sites by a recombinant *E. coli* enzyme in vitro. tRNase Zs from *Bacillus subtilis* and *Thermotoga maritima* also cleaved various unstructured RNAs. The *E. coli* and *B. subtilis* enzymes seem to have a tendency to cleave after cytidine or before uridine, while cleavage by the *T. maritima* enzyme inevitably occurred after CCA in addition to the other cleavages. Assays to determine optimal conditions indicated that metal ion requirements differ between *B. subtilis* and *T. maritima* tRNase Zs. There was no significant difference in the observed rate constant between unstructured RNA and pre-tRNA substrates, while the K_d value of a tRNase Z/unstructured RNA complex was much higher than that of an enzyme/pre-tRNA complex. Furthermore, eukaryotic tRNase Zs from yeast, pig, and human cleaved unstructured RNA at multiple sites, but an archaeal tRNase Z from *Pyrobaculum aerophilum* did not.

tRNase Z[1] (or 3′ tRNase; EC 3.1.26.11) exists in almost all cells and is believed to be working primarily for tRNA 3′ maturation (*1−6*). Usually, this enzyme cleaves off a 3′ trailer from pre-tRNA after the discriminator nucleotide, onto which the CCA residues are appended by tRNA nucleotidyltransferase, but exceptionally, *Thermotoga maritima* tRNase Z cleaves pre-tRNAs containing the $^{74}CCA^{76}$ sequence precisely after the A^{76} residue to create the mature 3′-termini (*4*). tRNase Zs can be divided into two groups: a short form (tRNase Z[S]) that consists of 300−400 amino acids and a long form (tRNase Z[L]) that contains of 800−900 amino acids (*7, 8*). Bacteria and archaea genomes contain a tRNase Z[S] gene only, while eukaryotic genomes encode either only tRNase Z[L] or both forms.

The C-terminal half region of tRNase Z[L] has high similarity to the whole region of tRNase Z[S], and these regions contain a well-conserved histidine motif, which has been shown to be essential for the tRNase Z activity in the *T. maritima*, *Drosophila melanogaster*, and *Arabidopsis thaliana* enzymes (*4, 9, 10*). Sequence analysis has suggested that tRNase Zs belong to the metallo-β-lactamase superfamily, and crystal structures of *T. maritima* and *Bacillus subtilis* tRNase Z[S]'s have revealed a four-layer $\alpha\beta/\beta\alpha$ sandwich fold that is typically found in metallo-β-lactamases (*11, 12*). In the crystal structures, these tRNase Z[S]'s existed as a homodimer, and metal ion(s) were coordinated in the catalytic center including the histidine motif. Models for pre-tRNA docking are proposed, in which one or two pre-tRNA molecules bind a positively charged surface of the enzyme dimer.

The genomes of human and *A. thaliana* contain both tRNase Z[S] and tRNase Z[L] genes, raising a curious question whether the short and long forms play differential roles in the cells. The fact that tRNase Z[L] is ~2-fold larger than tRNase Z[S] and has the extra N-terminal region that is dispensable for the pre-tRNA processing reaction implies that the long form might have an additional role (*3*). Indeed, only tRNase Z[L] can function as a four-base-recognizing RNA cutter (RNase 65) through a relatively stable complex between the enzyme and a 3′-truncated tRNA, although little is known about the physiological role and substrate of RNase 65 (*13*). Micro-pre-tRNA, which lacks the anticodon and D arms, and short double-stranded RNA are substrates of tRNase Z[L] but not of tRNase Z[S] (*8, 14*). Interestingly, human tRNase Z[L] has been shown to interact physically with the γ-tubulin complex, although a physiological significance is not clear (*15*).

The genome of *Saccharomyces cerevisiae* contains a tRNase Z[L] gene only, which is essential for viability (*16*). Because yeast seems to have a backup system using exoribonuclease(s) to remove pre-tRNA 3′ trailers (*17*), this suggests that yeast tRNase Z[L] may play another role other than pre-tRNA processing. In contrast, the *Escherichia coli* genome has genes for the five exoribonucleases in addition to tRNase Z (or RNase BN) that are involved in the removal of 3′ trailers to generate the CCA termini (*18, 19*), and the tRNase Z gene appears to be dispensable under normal growth conditions (*20*). *E. coli* tRNase Z, which cleaves pre-
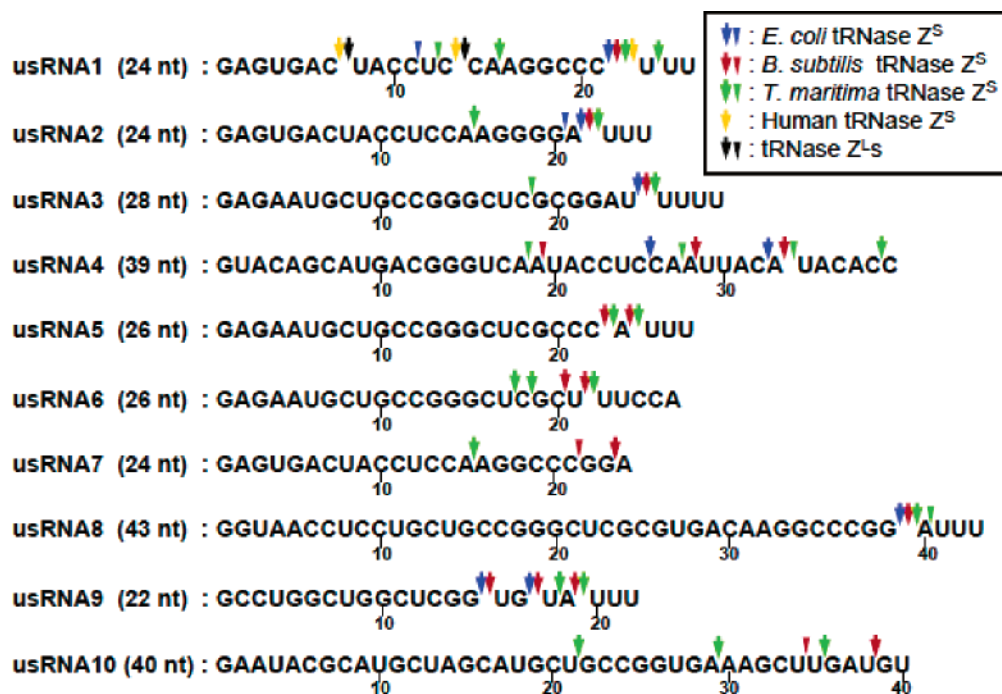
FIGURE 1: Unstructured RNA substrates. Major and minor cleavage sites at 52 °C in the presence of Mn^{2+} by tRNase Z^Ss from *E. coli* (blue), *B. subtilis* (red), *T. maritima* (green), and human (yellow) and tRNase Z^Ls (black) from yeast, pig, and human are indicated by arrows and arrowheads, respectively. The cleavage sites of usRNA1 by *B. subtilis* and *T. maritima* tRNase Zs were different from those under some different conditions (Figure 4). Very minor cleavage sites are omitted.

tRNAs after the discriminator (*4*), is essential for 3′ maturation of T4 bacteriophage pre-tRNAs that lack the CCA sequence like eukaryotic pre-tRNAs (*21*). However, the idea that tRNase Z is preserved during evolution to prepare for T4 bacteriophage infection would not be easy to accept.

We have been thinking of a possibility that *E. coli* tRNase Z might cleave RNAs other than pre-tRNAs for processing and/or degradation under some stress conditions. Here, we investigated whether unstructured RNA can be cleaved by *E. coli* tRNase Z and several other tRNase Zs and found that tRNase Zs indeed cleave various unstructured RNAs in vitro.

MATERIALS AND METHODS

Construction of an Expression Plasmid for B. subtilis tRNase Z. The full-length coding region (927 bp) for *B. subtilis* tRNase Z was PCR-amplified from its genome. The primer pair 5′-GGATCCATGGAATTACTTTTTTTAGG-3′ and 5′-AAGCTTTTATCAGCCTCGCGGGACGTTTA-3′ was used. The amplified gene was cloned between the *Bam*H I and *Hind* III sites of pQE-80L (Qiagen). We confirmed that the insert region is the same as the published sequence (GenBank accession no.: Z99116).

Expression and Purification of tRNase Z. Pig tRNase Z^L was purified from liver as described (*22*). Recombinant tRNase Z^S's from *E. coli*, *B. subtilis*, *T. maritima*, *Pyrobaculum aerophilum*, and humans and recombinant yeast and human tRNase Z^L's were generated from *E. coli* cells as described previously (*3*, *4*). The N-terminal half of human tRNase Z^L and the jellyfish green fluorescent protein were also produced from the pTYB11 (New England BioLabs)-based plasmids in the *E. coli* cells (*3*).

RNA Synthesis and Labeling. The RNAs were synthesized in vitro with T7 RNA polymerase (Promega) from the synthetic DNAs containing its promoter. The sequence of usRNA11 is 5′-GAGGAGUUGUGUAUUGUGGACGAA-GUACCGAAAGGUCUUACCGGAAAACUCGACGCAAGAAAAA-UCAGUAGAGAUCCUCAUAAAGGCCAAGAAGGGCGGAAA-GAUCGCCGUGUAAUUCUAGAUCAUAGACCUGUACAAUGC-UGCUGGCCGGCCGCUUCGAGCAGACAUGAUAAGAUACA-UUG-3′. The other RNA sequences are shown in Figure 1. Computer calculation for these substrates using mfold predicted no stable structures with the free energy ΔG of less than -10 kcal/mol with the exception of usRNA8 (-13.5 kcal/mol) and usRNA11 (-46.6 kcal/mol) (*23*). The transcription reactions were carried out under the conditions recommended by the manufacturer (Promega), and the transcribed RNAs were gel-purified.

The transcribed RNAs were labeled with fluorescein according to the manufacturer's protocol (Amersham Pharmacia Biotech). Briefly, after the removal of the 5′-phosphates of the transcripts with bacterial alkaline phosphatase (Takara Shuzo), the transcripts were phosphorylated using ATPγS and T4 polynucleotide kinase (Takara Shuzo). Then, a single fluorescein moiety was added onto the 5′-phosphorothioate site. The labeled RNAs were gel-purified before assays.

3′-Fluorescein-labeled usRNA2 without a 5′-phosphate was synthesized with a DNA/RNA synthesizer and purified through high-performance liquid chromatography (Nippon Bioservice).

In Vitro RNA Cleavage Assay. The RNA cleaving reactions for fluorescein-labeled RNAs were performed with tRNase Zs of various origins in a mixture (6 μL) containing $0-50$ mM $MnCl_2$, $0-20$ mM $MgCl_2$, $0-90$ mM NaCl, or $0-200$ mM spermidine in addition to 10 mM Tris-HCl (pH 8) and 1.5 mM dithiothreitol. In pre-tRNA competition assays, unlabeled pre-tRNA ($0.028-2.8$ μM) was also added.
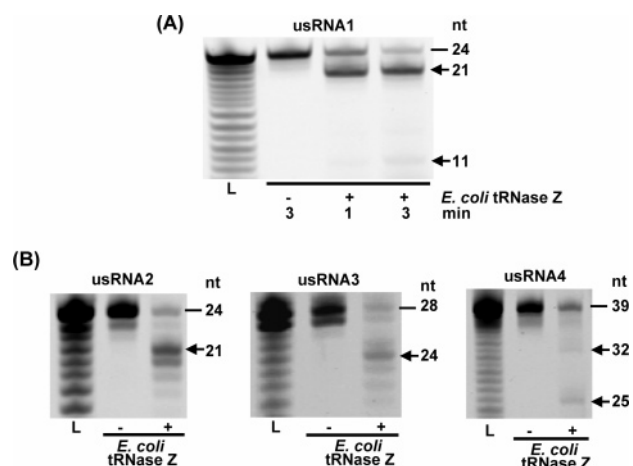
FIGURE 2: Assays for *E. coli* tRNase Z cleavages of the 5′-fluorescein-labeled unstructured RNAs usRNA1−4. The products were analyzed on a 20% polyacrylamide−8 M urea gel. An RNA substrate and primary 5′ cleavage products are indicated by a bar and arrows, respectively. L denotes an alkaline ladder of the fluorescein-labeled substrate. (A) usRNA1 (2 pmol) was reacted in the presence of 1 mM $MnCl_2$ with the enzyme (10 pmol) at 52 °C for the indicated time. (B) usRNA2−4 (2 pmol) were incubated under the same conditions for 2 min. The substrate band of the precise length among the 3′-heterogeneous transcript bands from the intrinsic property of T7 RNA polymerase was identified by comparison with a size standard.

FIGURE 3: Cleavage assays for 5′-fluorescein-labeled usRNA1−4 with *B. subtilis* and *T. maritima* tRNase Zs. The products were analyzed on a 20% polyacrylamide−8 M urea gel. An RNA substrate and primary 5′ cleavage products are indicated by a bar and arrows, respectively. L denotes an alkaline ladder of the fluorescein-labeled substrate. (A) usRNA1 (2 pmol) was reacted in the presence of 1 mM $MnCl_2$ with *B. subtilis* or *T. maritima* tRNase Z (10 pmol) at 52 °C for the indicated time. (B) usRNA2−4 (2 pmol) were incubated under the same conditions for 2 min. The substrate band of the precise length among the 3′-heterogeneous transcript bands from the intrinsic property of T7 RNA polymerase was identified by comparison with a size standard.

Temperature, reaction time, and amounts of substrate RNAs and tRNase Zs changed depending on assays and are specified in the figure legends. After resolution of the reaction products on a 10 or 20% polyacrylamide−8 M urea gel, the gel was analyzed with a Typhoon 9210 (Amersham Pharmacia Biotech).

Gel-Shift Analysis. To determine the dissociation constant of a tRNase Z/substrate complex, the fluorescein-labeled RNA substrate (0.18−1.8 pmol) was incubated on ice for 10 min with various amounts (0.6−320 pmol) of tRNase Z in a buffer (6 μL) containing 10 mM Tris-HCl (pH 7.5), 1.5 mM dithiothreitol, and 1 mM $MnCl_2$ (22). After incubation, the sample was mixed with the same volume of a loading buffer (10 mM Tris-HCl, pH 7.5, 1 mM EDTA, and 50% glycerol) and electrophoresed on a 5% nondenaturing polyacrylamide gel with TBE buffer (90 mM Tris base, 90 mM boric acid, and 1.5 mM EDTA, pH 8.3). After electrophoresis, the labeled RNAs were quantitated with the Typhoon 9210.

RESULTS AND DISCUSSION

E. coli tRNase Z Cleaves Unstructured RNA Substrates. First, we tested a 24-nt unstructured RNA, usRNA1 (Figure 1), for in vitro cleavage by *E. coli* histidine-tagged tRNase Z. usRNA1 was 5′-end-labeled with fluorescein and incubated at 52 °C with the enzyme in the presence of Mn^{2+}. Surprisingly, this substrate was cleaved by the enzyme very efficiently after cytidine at the 21st nt and slightly after cytidine at the 11th nt (Figure 2A). The three other 5′-fluorescein-labeled unstructured RNAs usRNA2−4 of 24−39 nt (Figure 1) were also examined, and all these substrates were cleaved (Figure 2B). Likewise, two more substrates, 43-nt usRNA8 and 22-nt usRNA9, were cleaved by the enzyme (Figure 1 and Figure S1 of the Supporting
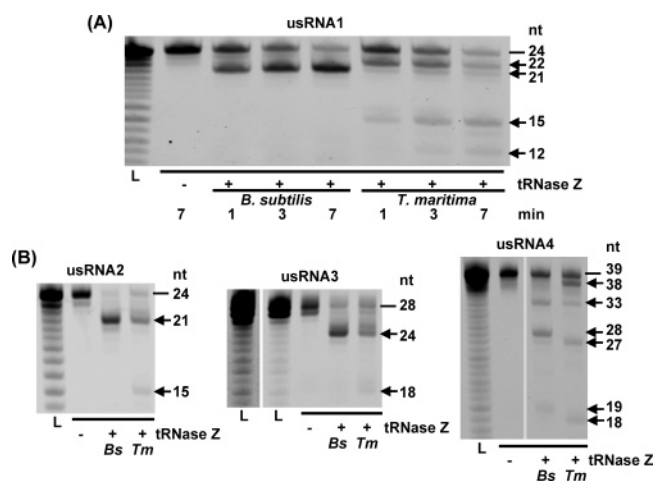
Information). These results indicate that *E. coli* tRNase Z can also cleave RNA other than pre-tRNA.

Various Unstructured RNAs Are Substrates for tRNase Zs from B. subtilis and T. maritima. To determine whether unstructured RNA cleavages occur by other tRNase Zs, we tested two eubacterial tRNase Zs from *B. subtilis* and *T. maritima* for cleavage of usRNA1. Both enzymes cleaved usRNA1 very efficiently but at different sites (Figure 3A). The major cleavage site by the *B. subtilis* enzyme was the same as that by the *E. coli* one, but the minor cleavage after the 11th nt was not detected under the conditions described in the legend to Figure 3. *T. maritima* tRNase Z cleaved usRNA1 at several sites (Figure 1).

As shown in Figure 3B, 5′-fluorescein-labeled usRNA2−4 were also cleaved by both tRNase Zs (Figure 1). Furthermore, the six other unstructured RNAs, usRNA5−10, were examined for cleavages by both enzymes, and all of these substrates were also cleaved in most cases at multiple sites with various efficiencies (Figure S2 of the Supporting Information). The cleavage sites by the *B. subtilis* enzyme were nearly identical to those by the *E. coli* enzyme, while substrate cleavage patterns by the *T. maritima* enzyme were different from those by the former two enzymes in most substrates. Interestingly, when substrates contain the CCA sequence, cleavage by *T. maritima* tRNase Z inevitably occurred after CCA in addition to the other cleavages (Figure 1). From these results, we concluded that eubacterial tRNase Zs can generally cleave unstructured RNAs.

tRNase Z Cleaves Substrates Endoribonucleolytically. To confirm that tRNase Z cleaves unstructured RNA endoribonucleolytically as it cleaves pre-tRNA, we performed the cleavage assays for the 24-nt 3′-fluorescein-labeled usRNA2. In the assay using *T. maritima* tRNase Z, a 3-nt 3′ cleavage product was detected (Figure S3 of the Supporting Informa-

tion). The presence of this 3-nt product, together with the above observation that the *T. maritima* enzyme generated primarily the 21-nt 5′ cleavage product from the 24-nt 5′-fluorescein-labeled usRNA2 (Figure 3B), suggests that the cleavage occurs endoribonucleolytically. The reason we hardly detected a 9-nt 3′ cleavage product that abuts on the 15-nt 5′ cleavage product would be because the second cleavage of the 9-nt 3′ cleavage product by the enzyme occurred easily at the 21st nt to generate the 3-nt 3′ cleavage product (Figures 3B and S3 of the Supporting Information)

Similarly, *E. coli* and *B. subtilis* tRNase Zs produced the 3-nt 3′ cleavage product from the 3′-fluorescein-labeled usRNA2, implying that both tRNase Zs cleave usRNA2 endoribonucleolytically (Figures 2B, 3B, and S3 of the Supporting Information). In the assays with these two enzymes, 1- and 2-nt 3′ cleavage products were also detected (Figure S3 of the Supporting Information). These additional products would have been generated by further cleavages of the 3-nt 3′ cleavage product or by the first cleavages of the 24-nt full-length substrate. In the latter case, the reason we could hardly detect the corresponding 23- and 22-nt 5′ cleavage products (Figures 2B and 3B) would be because these 5′ products were further cleaved to generate the 21-nt 5′ product that was primarily detected.

Metal Ion Requirements Differ between B. subtilis and T. maritima tRNase Zs. To determine optimal conditions for the unstructured RNA cleavages, we assayed *B. subtilis* and *T. maritima* tRNase Zs for usRNA1 cleavage by varying a concentration of $MnCl_2$, $MgCl_2$, NaCl, or spermidine, or by varying temperature. The *B. subtilis* enzyme was highly active within the range of 0−50 mM $MnCl_2$ and the most active around 1−5 mM, while the activity of *T. maritima* tRNase Z was the highest at 0.05 mM and was lost without $MnCl_2$ (Figure 4A). With respect to $MgCl_2$, the activity of *B. subtilis* tRNase Z was very high at 0−0.2 mM, but became very weak at more than 3 mM generating an additional 13-nt product, although the *T. maritima* enzyme was almost inactive within the tested range (Figure 4B). The major 21-nt product by the *B. subtilis* enzyme was generated most efficiently around 6 mM NaCl, and the additional 13-nt product became prominent around 90 mM, while only the 13-nt product by the *T. maritima* enzyme was faintly detected within the tested range (Figure 4C). On the whole, dependence on metal ions of the unstructured RNA cleavages was quite different from that of pre-tRNA cleavages by *E. coli* and *T. maritima* tRNase Zs (*8*).

Generally, the coordination of Zn^{2+} or Mn^{2+} ions in the active site including the histidine motif appears to be essential for the activities of metallo-β-lactamase superfamily enzymes (*24*, *25*), and Mg^{2+} or Mn^{2+} ions appear to be needed for the proper folding of pre-tRNA and/or the efficient tRNase Z/pre-tRNA interaction. The reason Mg^{2+} ions were hardly able to make the *T. maritima* enzyme cleave the substrate may be because the enzyme has difficulty in holding the endogenous Zn^{2+} or Mn^{2+} ions in the active center bound by unstructured RNA and because the Mg^{2+} ions cannot be coordinated in the center. In contrast, even Mg^{2+} ions activated the *B. subtilis* enzyme probably due to tight binding of the endogenous Zn^{2+} or Mn^{2+} ions to the catalytic center. The Zn^{2+} ions alone hardly supported the activity of tRNase Z to cleave unstructured RNA (data not shown), confirming the importance of the Mg^{2+} and Mn^{2+} ions mentioned above.
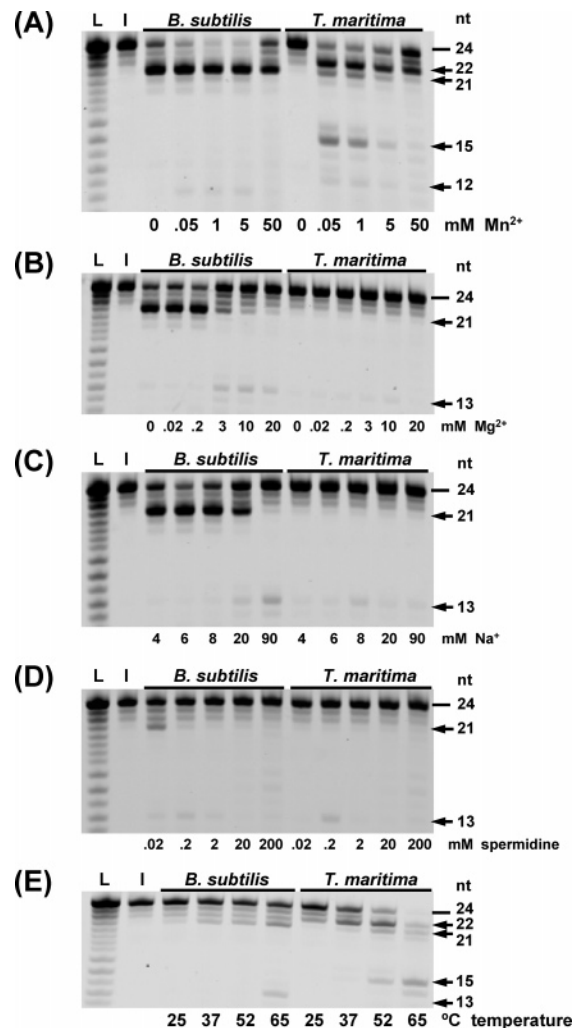

FIGURE 4: Optimal conditions for 5′-fluorescein-labeled usRNA1 cleavages by *B. subtilis* and *T. maritima* tRNase Zs. usRNA1 (2 pmol) was reacted with *B. subtilis* or *T. maritima* tRNase Z (10 pmol) at 52 °C for 2 min in the presence of various concentrations of $MnCl_2$ (A), $MgCl_2$ (B), NaCl (C), or spermidine (D). The substrate was also incubated in the presence of 1 mM $MnCl_2$ at various temperatures (E). The products were analyzed on a 20% polyacrylamide−8 M urea gel. An RNA substrate and primary 5′ cleavage products are indicated by a bar and arrows, respectively. L, an alkaline ladder of the fluorescein-labeled substrate; I, input substrate RNA.

In the presence of spermidine, the 13-nt product by *T. maritima* tRNase Z slightly appeared only at 0.2 mM, and the cleavage after the 21st nt by the *B. subtilis* enzyme was strongly inhibited within the range of 0.02−200 mM (Figure 4D). This inhibitory effect may be due to substrate RNA folding with the help of spermidine. To examine temperature dependence of the activity, we preincubated an enzyme at a reaction temperature for 10 min, added the RNA substrate to an enzyme mix, and further incubated at the same temperature for 2 min. As shown in Figure 4E, the activities of both enzymes increased with the increase in temperature at least up to 65 °C. In this paper, we performed most of the assays for *B. subtilis* and *E. coli* tRNase Zs at 52 °C, which is far from the physiological temperatures, because this is near the optimal temperatures. We note, however, that the *B. subtilis* (Figure 4E) and *E. coli* (data not shown) enzymes have some cleavage activities also at 37 °C.

Table 1: Observed Rate Constants and Dissociation Constants for TRNase Z

tRNase Z	substrate	k_{obs} (min^{-1})[a]	K_d (μM)[b]
B. subtilis	usRNA1	0.61 ± 0.04	25 ± 14
	pre-tRNA^{Cys}	0.26 ± 0.02	3.1 ± 0.7
T. maritima	usRNA1	0.19 ± 0.02	$\sim$300
	pre-tRNA^{Arg}	0.33 ± 0.04	0.22 ± 0.08

[a] A total of 0.17 μM of usRNA1, *B. subtilis* pre-tRNA^{Cys}, or *T. maritima* pre-tRNA^{Arg} was assayed at 52 °C for 1.5 min using 1.7 μM of tRNase Z in the presence of 1 mM MnCl$_2$. Data are the means $\pm$ SD of three independent experiments. [b] The K_d values were calculated based on the gel-shift data (Figure S4 of the Supporting Information). The K_d value for the *T. maritima* tRNase Z/usRNA1 complex was too big to determine accurately. Data are the means $\pm$ SD of three independent experiments.

Affinity of Unstructured RNA to tRNase Z Is Much Lower Than That of Pre-tRNA. We measured the observed rate constant k_{obs} for the usRNA1 cleavage under single-turnover conditions and the dissociation constant K_d of a tRNase Z/usRNA1 complex. The k_{obs} value for the *B. subtilis* enzyme was ~3-fold bigger than that for the *T. maritima* enzyme, and these k_{obs} values were ~2-fold greater and smaller, respectively, than those for pre-tRNA cleavages (Table 1). These results suggest that there would be no significant difference in the mechanism of the phosphodiester cleavage step between unstructured RNA and pre-tRNA substrates and between the enzymes. In contrast, the K_d values of tRNase Z/usRNA1 complexes were ~10-fold and ~1000-fold, respectively, higher than those of enzyme/pre-tRNA complexes (Table 1 and Figure S4 of the Supporting Information). These much higher K_d values would explain why we have been unable to detect cleavages in the unstructured distal region of pre-tRNA trailers (*4*). Although in this study we used 5 or 10 times higher amounts of the enzymes than those of the substrates, we confirmed that ~10 times less amounts of the enzymes than those of the substrates can also cleave the substrates (data not shown).

Long RNA Is Also a Substrate for tRNase Z. If the activity to cleave unstructured RNAs is for processing and/or degradation of mRNAs, tRNase Zs should be able to cleave relatively long RNAs. To test this, we assayed a 182-nt RNA, usRNA11, for cleavages by *B. subtilis* and *T. maritima* tRNase Zs. Even this long RNA was cleaved at multiple sites by both enzymes (Figure 5). Although we did not determine the exact cleavage sites, the cleavage patterns clearly differed between the enzymes. Notably, usRNA11 contains a single CCA sequence at the 87−89 nt, and *T. maritima* tRNase Z appeared to cleave it after the A residue, albeit inefficiently, from the comparison with the 93-nt size standard.

Eukaryotic tRNase Z Cleaves Unstructured RNA, but Archaeal tRNase Z Does Not. To see whether eukaryotic and archaeal tRNase Zs can also cleave unstructured RNA, we tested *P. aerophilum* tRNase Z; human tRNase Z^S; and yeast, pig, and human tRNase Z^L for usRNA1 cleavage in the presence of Mn^{2+} or Mg^{2+}. These enzymes, except for the *P. aerophilum* enzyme, processed usRNA1 at multiple sites (Figures 1 and 6). The eukaryotic tRNase Zs cleaved this substrate commonly after the 13th and 7th nt, and human tRNase Z^S additionally cut it after the 21st only in the presence of Mn^{2+} as *E. coli* and *B. subtilis* tRNase Zs did (Figures 1 and 6).
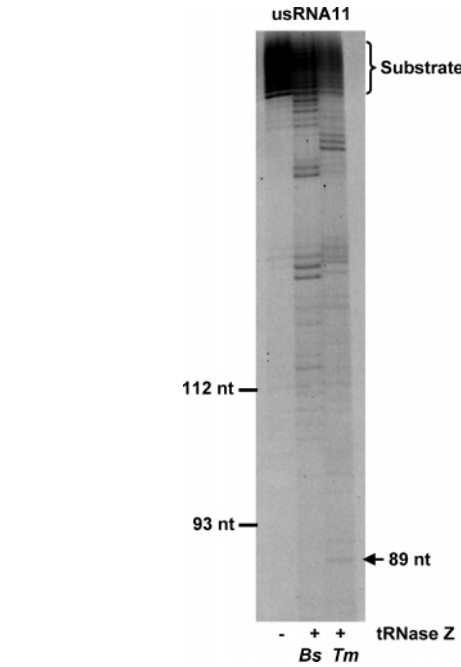

FIGURE 5: Cleavage assays for the long RNA usRNA11 with *B. subtilis* and *T. maritima* tRNase Zs. The substrate (2 pmol) was incubated with an enzyme (10 pmol) in the presence of 1 mM MnCl$_2$ at 52 °C for 3 min. The products were analyzed on a 10% polyacrylamide−8 M urea gel. Size standards and the cleavage product at the CCA sequence are indicated by bars and an arrow, respectively. The heterogeneity of usRNA11 is due to the 3′-heterogeneity from the intrinsic property of T7 RNA polymerase.
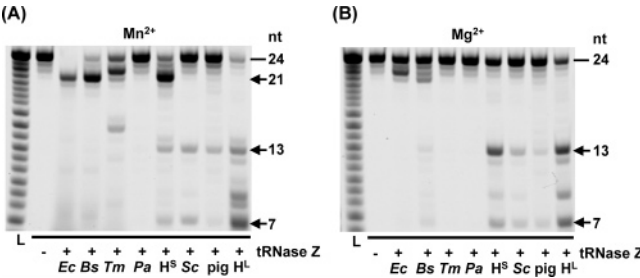

FIGURE 6: Assays for usRNA1 cleavages by eukaryotic and archaeal tRNase Zs. The substrate (2 pmol) was incubated in the presence of 1 mM MnCl$_2$ (A) or 3.3 mM MgCl$_2$ (B) with an enzyme (2 pmol) at 52 °C for 2 min. The products were analyzed on a 20% polyacrylamide−8 M urea gel. An RNA substrate and primary 5′ cleavage products are indicated by a bar and arrows, respectively. L denotes an alkaline ladder of the fluorescein-labeled substrate. *Ec*, *E. coli* tRNase Z; *Bs*, *B. subtilis* tRNase Z; *Tm*, *T. maritima* tRNase Z; *Pa*, *P. aerophilum* tRNase Z; H^S, human tRNase Z^S; *Sc*, *Saccharomyces cerevisiae* tRNase Z^L; pig, pig tRNase Z^L; H^L, human tRNase Z^L.

The Activity Indeed Originated from tRNase Z. Although we showed that recombinant tRNase Zs from various species can cleave various unstructured RNA substrates other than pre-tRNAs in vitro, there was a possibility that the activities were originated from contaminating *E. coli* nucleases. To exclude this possibility, we examined two different samples prepared from *E. coli* cells containing the expression plasmid pQE-80L or pTYB11without tRNase Z cDNAs for usRNA2 cleavage, and we could hardly detect cleavage products (Figure S5 of the Supporting Information). In addition, an unrelated protein, green fluorescent protein, and the N-terminal half of human tRNase Z^L that cannot cleave even pre-tRNAs (*3*), which were prepared through the pTYB11
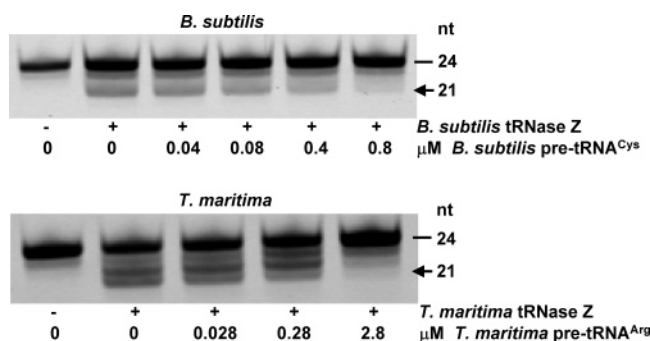
FIGURE 7: Pre-tRNA competition assays. The 5′-fluorescein-labeled usRNA2 (2 pmol) was incubated with *B. subtilis* or *T. maritima* tRNase Z (10 pmol) in the presence of 1 mM MnCl$_2$ and various amounts of unlabeled pre-tRNA at 52 °C for 2 min. The products were analyzed on a 20% polyacrylamide−8 M urea gel. An RNA substrate and primary 5′ cleavage products are indicated by a bar and arrows, respectively.

and pQE-80L expression systems, respectively, did not show the activity (Figure S5 of the Supporting Information).

Furthermore, we performed competition assays for *B. subtilis* and *T. maritima* tRNase Zs using unlabeled pre-tRNAs, and we observed that the levels of usRNA2 cleavage products decreased with the increase in the amount of pre-tRNAs (Figure 7). This observation implies that tRNase Z, whose genuine substrate is pre-tRNA, is the enzyme that cleaves unstructured RNA. Also, *T. maritima* tRNase Z, which was treated at 80 °C for 20 min to remove contaminating *E. coli* proteins in the course of preparation, still showed the activity to cleave unstructured RNAs. Taken together, these observations would rule out the possibility of *E. coli* nuclease contamination and would confirm that unstructured RNAs are substrates of tRNase Zs.

Cleavage Site Selection and a Mechanism for Unstructured RNA Recognition. The major cleavage sites of the unstructured RNA substrates tested here were nearly identical between *E. coli* and *B. subtilis* tRNase Zs (Figure 1). Although we did not recognize a consensus sequence around the cleavage sites, the enzymes seem to have a tendency to cleave after cytidine or before uridine. A pre-tRNA docking model for *B. subtilis* tRNase Z suggests that the enzyme recognizes pre-tRNA through the interactions between the positively charged flexible arm and the T-arm and between the positively charged surface near the active site and the acceptor stem (*12*). Because it is unlikely that the enzyme clamps unstructured RNA through the flexible arm, the unstructured RNA would bind to the positively charged central region. The ~10-fold larger K_d value will be due to this restricted interaction. The scissile nucleotide preference would be explained by the properties of active site amino acid residues interacting with the scissile nucleotide. Similarly, *E. coli* tRNase Z would interact with unstructured RNA since both enzymes have a high sequence similarity.

In contrast, *T. maritima* tRNase Z showed a sequence preference; it cleaved the unstructured substrates inevitably after the CCA sequence just like it cleaved *T. maritima* pre-tRNAs (*4*). This would be most likely due of the interaction with the CCA-binding domain in the catalytic center (*4*). In addition, the unstructured RNA would bind to the positively charged surface of the enzyme like the *B. subtilis* enzyme (*11*).

tRNase Z^L's, regardless of their origins, cleaved the unstructured RNA usRNA1 at the same sites, and the cleavages occurred after cytidine. The difference in cleavage pattern from eubacterial tRNase Zs could be attributed to an interaction with the additional N-terminal half domain or, alternatively, with an unidentified eukaryote-specific motif in the C-terminal half domain, because the cleavage pattern of human tRNase Z^S was a composite of eubacterial and eukaryotic long form patterns. Further analysis of this interesting difference in cleavage pattern among prokaryotic tRNase Z^S, eukaryotic tRNase Z^S, and tRNase Z^L might provide insights into the evolutionary relationship of these tRNase Zs and into a possible differential role between the long and short forms of human tRNase Z.

SUPPORTING INFORMATION AVAILABLE

Assays for *E. coli* tRNase Z cleavages of usRNA8 and usRNA9 (Figure S1), cleavage assays for usRNA5−10 with *B. subtilis* and *T. maritima* tRNase Zs (Figure S2), assays showing endoribonucleolytic cleavage of unstructured RNA by tRNase Z (Figure S3), gel-shift analysis (Figure S4), and assays to exclude the possibility of *E. coli* nuclease contamination (Figure S5). This material is available free of charge via the Internet at http://pubs.acs.org.

REFERENCES

1. Mörl, M., and Marchfelder, A. (2001) The final cut. The importance of tRNA 3′-processing, *EMBO Rep. 2*, 17−20.
2. Schiffer, S., Rosch, S., and Marchfelder, A. (2002) Assigning a function to a conserved group of proteins: the tRNA 3′-processing enzymes, *EMBO J. 21*, 2769−2777.
3. Takaku, H., Minagawa, A., Takagi, M., and Nashimoto, M. (2003) A candidate prostate cancer susceptibility gene encodes tRNA 3′ processing endoribonuclease, *Nucleic Acids Res. 31*, 2272−2278.
4. Minagawa, A., Takaku, H., Takagi, M., and Nashimoto, M. (2004) A novel endonucleolytic mechanism to generate the CCA 3′ termini of tRNA molecules in *Thermotoga maritima*, *J. Biol. Chem. 279*, 15688−15697.
5. Dubrovsky, E. B., Dubrovskaya, V. A., Levinger, L., Schiffer, S., and Marchfelder, A. (2004) *Drosophila* RNase Z processes mitochondrial and nuclear pre-tRNA 3′ ends in vivo, *Nucleic Acids Res. 32*, 255−262.
6. Schilling, O., Späth, B., Kostelecky, B., Marchfelder, A., Meyer-Klaucke, W., and Vogel, A. (2005) Exosite modules guide substrate recognition in the ZiPD/ElaC protein family, *J. Biol. Chem. 280*, 17857−17862.
7. Tavtigian, S. V., Simard, J., Teng, D. H., Abtin, V., Baumgard, M., Beck, A., Camp, N. J., Carillo, A. R., Chen, Y., Dayananth, P., Desrochers, M., Dumont, M., Farnham, J. M., Frank, D., Frye, C., Ghaffari, S., Gupte, J. S., Hu, R., Iliev, D., Janecki, T., Kort, E. N., Laity, K. E., Leavitt, A., Leblanc, G., McArthur-Morrison, J., Pederson, A., Penn, B., Peterson, K. T., Reid, J. E., Richards, S., Schroeder, M., Smith, R., Snyder, S. C., Swedlund, B., Swensen, J., Thomas, A., Tranchant, M., Woodland, A. M., Labrie, F., Skolnick, M. H., Neuhausen, S., Rommens, J., and Cannon-Albright, L. A. (2001) A candidate prostate cancer susceptibility gene at chromosome 17p, *Nat. Genet. 27*, 172−180.
8. Takaku, H., Minagawa, A., Takagi, M., and Nashimoto, M. (2004) The N-terminal half-domain of the long form of tRNase Z is required for the RNase 65 activity, *Nucleic Acids Res. 32*, 4429−4438.
9. Zareen, N., Yan, H., Hopkinson, A., and Levinger, L. (2005) Residues in the conserved His domain of fruit fly tRNase Z that function in catalysis are not involved in substrate recognition or binding, *J. Mol. Biol. 350*, 189−199.
10. Spath, B., Kirchner, S., Vogel, A., Schubert, S., Meinlschmidt, P., Aymanns, S., Nezzar, J., and Marchfelder, A. (2005) Analysis of the functional modules of the tRNA 3′ endonuclease (tRNase Z), *J. Biol. Chem. 280*, 35440−35447.

11. Ishii, R., Minagawa, A., Takaku, H., Takagi, M., Nashimoto, M., and Yokoyama, S. (2005) Crystal structure of the tRNA 3′ processing endoribonuclease tRNase Z from *Thermotoga maritima*, *J. Biol. Chem. 280*, 14138−14144.

12. de la Sierra-Gallay, I. L., Pellegrini, O., and Condon, C. (2005) Structural basis for substrate binding, cleavage and allostery in the tRNA maturase RNase Z, *Nature 433*, 657−661.

13. Nashimoto, M. (1995) Conversion of mammalian tRNA 3′ processing endoribonuclease to four-base-recognizing RNA cutters, *Nucleic Acids Res. 23*, 3642−3647.

14. Shibata, H. S., Takaku, H., Takagi, M., and Nashimoto, M. (2005) The T loop structure is dispensable for substrate recognition by tRNase ZL, *J. Biol. Chem. 280*, 22326−22334.

15. Korver, W., Guevara, C., Chen, Y., Neuteboom, S., Bookstein, R., Tavtigian, S., and Lees, E. (2003) The product of the candidate prostate cancer susceptibility gene *ELAC2* interacts with the γ-tubulin complex, *Int. J. Cancer 104*, 283−288.

16. Chen, Y., Beck, A., Davenport, C., Chen, Y., Shattuck, D., and Tavtigian, S. V. (2005) Characterization of *TRZ1*, a yeast homolog of the human candidate prostate cancer susceptibility gene ELAC2 encoding tRNase Z, *BMC Mol. Biol. 6*, 12.

17. Yoo, C. J., and Wolin, S. L. (1997) The yeast La protein is required for the 3′ endonucleolytic cleavage that matures tRNA precursors, *Cell 89*, 393−402.

18. Li, Z., and Deutscher, M. P. (1996) Maturation pathways for *E. coli* tRNA precursors: a random multienzyme process in vivo, *Cell 86*, 503−512.

19. Ezraty, B., Dahlgren, B., and Deutscher, M. P. (2005) The RNase Z homologue encoded by *Escherichia coli elaC* gene is RNase BN, *J. Biol. Chem. 280*, 16542−16545.

20. Schilling, O., Ruggeberg, S., Vogel, A., Rittner, N., Weichert, S., Schmidt, S., Doig, S., Franz, T., Benes, V., Andrews, S. C., Baum, M., and Meyer-Klaucke, W. (2004) Characterization of an *Escherichia coli elaC* deletion mutant, *Biochem. Biophys. Res. Commun. 320*, 1365−1373.

21. Seidman, J. G., Schmidt, F. J., Foss, K., and McClain, W. H. (1975) A mutant of *Escherichia coli* defective in removing 3′ terminal nucleotides from some transfer RNA precursor molecules, *Cell 5*, 389−400.

22. Nashimoto, M., Nashimoto, C., Tamura, M., Kaspar, R. L., and Ochi, K. (2001) The inhibitory effect of the autoantigen La on in vitro 3′ processing of mammalian precursor tRNAs, *J. Mol. Biol. 312*, 975−984.

23. Zuker, M. (2003) Mfold web server for nucleic acid folding and hybridization prediction, *Nucleic Acids Res. 31*, 3406−3415.

24. Vogel, A., Schilling, O., Niecke, M., Bettmer, J., and Meyer-Klaucke, W. (2002) *ElaC* encodes a novel binuclear zinc phosphodiesterase, *J. Biol. Chem. 277*, 29078−29085.

25. Schilling, O., Wenzel, N., Naylor, M., Vogel, A., Crowder, M., Makaroff, C., and Meyer-Klaucke, W. (2003) Flexible metal binding of the metallo-β-lactamase domain: glyoxalase II incorporates iron, manganese, and zinc in vivo. *Biochemistry 42*, 11777−11786.